those of pulse A. In the case of copper-activated phosphors the pulse shape of B is very similar to that of A and is about 180° out of phase with respect to A. The voltage and light sum per pulse curve is reminiscent of the voltage to current relationship of a space-charge-saturated diode. In the case of silver-activated phosphors, pulse A leads pulse B by about 90°. With increase of the voltage the pulse width gets broader and the amplitude larger (the width getting relatively wider than the corresponding increase of the amplitude). Pulse B is probably a function of the impurities in the phosphor.

There are similarities between the effects during the transitory period and those during phosphorescence. In both cases one observes rapid changes in the average brightness and always two amplitudes per cycle. For short persistent phosphors the transient effects during both phosphorescence and excitation are of short duration. Apparently this effect can be connected with emptying of traps. The subsequent quenching may also be related to changes in transition probabilities (or radiationless transitions) due to the influence of the electric field.

From the theory of Matossi[8] it follows that two pulses of equal amplitude per cycle should be observed. We found at some voltages only one pulse. Furthermore, as explained before, the different behavior of A and B proves that whenever there are two pulses per cycle, they are due to two different effects.

We think that the appearance of the two amplitudes suggests that surface effects are involved.

Experiments in electroluminescence have shown that there exist in general two pulses of light per cycle which are out of phase with voltage.[16-18] At certain voltages, two secondary light pulses are found about 90° out of phase with the main peaks.[16,19] For silver-activated phosphors, we found that the pulse B was about 90° out of phase with the pulse A, whereas for copper-activated phosphors B was about 180° out of phase. Zalm et al.[19] found no secondary light peaks for copper-activated phosphors. It is tempting to correlate the secondary peaks observed in electroluminescence with the pulses B observed during excitation. In this case, the nonobservance by Zalm et al. of the secondary peak in copper-activated phosphors in electroluminescence could possibly be explained by a masking of the secondary peak by the next main peak (because of about 180° phase shift). Apparently no such correlation can exist, however, between the main peaks in electroluminescence and the pulses A, as the former are emitted near the cathode[16] and the latter near the anode.

[16] W. W. Piper and F. E. Williams, Phys. Rev. 87, 191 (1952).
[17] J. F. Waymouth and F. Bitter, Phys. Rev. 95, 941 (1954).
[18] See also papers in reference 10.
[19] Zalm, Diemer, and Klasens, Philips Research Repts. 9, 81 (1954).

Paramagnetic Resonance Absorption in Glass*†

R. H. SANDS‡
Department of Physics, Washington University, St. Louis, Missouri
(Received March 2, 1955)

Paramagnetic resonance absorptions occurring with spectroscopic splitting factors of 4 and 6 were noted in all glass samples studied. These were apparently anisotropic g-values for a specific impurity and the peaks recorded are interpreted as being the result of a distribution of Stark fields over all directions in the glass. Resonances were also recorded having g-values near 2. Nearly all of these showed hyperfine structures characteristic of the known paramagnetic additions in the glasses. The absorption line observed for cupric ions in lattice modifying positions in a soda-lime-silica base glass has been quantitatively explained and the parameters compared favorably with those resulting for copper in the Tutton salts.

I. INTRODUCTION

CHANCE observations of paramagnetic resonance absorption in glass have led to a detailed study of such absorption in numerous glass samples of varying composition furnished by the Corning Glass Works, Corning, New York. The results have indicated possible applications of this technique to glass technology as well as in the study of the vitreous state.

It has long been known that if an atom has a partially filled electronic shell, there will exist a permanent electronic magnetic dipole moment. Hund's rules[1] and the Pauli exclusion principle allow one to predict the manner in which the electrons in the unfilled shell, with their intrinsic spins, will fill the available orbital angular momentum levels.

[1] F. Hund, *Linienspektren und periodisches System der Elemente* (Verlag Julius Springer, Berlin, 1927), p. 124.

When the atom or ion is placed in a lattice position in a solid, the surrounding diamagnetic neighbors produce an electrostatic potential at the ion in question. This potential causes a splitting of the orbital levels in accord with group theoretical considerations.[2] The magnitude of this Stark splitting varies with environment but is normally several thousand wave numbers for iron-group ions. Since this is much larger than the thermal energy (200 cm^{-1} at 300°K), one need consider only the ground state to first approximation. Should this ground state be a nondegenerate orbital state, then it must have the total spin degeneracy of the system (the splitting of the spin degeneracy is small). If the zero-order Stark interaction has such symmetry as to leave the ground orbital state degenerate, then this ground state will split according to the theorem of Jahn and Teller[3] leaving only the Kramers degeneracy. It is reasonable to conclude that the ground state will be a doublet if the number of electrons is odd and a singlet if the number is even (the next higher state usually being some 100 cm^{-1} away). For spin doublet ground states it has been shown by Pryce that the spin-orbit coupling between states and the electronic Zeeman interaction with an applied magnetic field H can be considered to give two ground-state energy levels:

$$E_{\pm} = \pm \tfrac{1}{2} g \mu_B H, \tag{1}$$

where $g = (g_{\shortparallel}{}^2 \cos^2\theta + g_{\perp}{}^2 \sin^2\theta)^{\frac{1}{2}}$, μ_B is the Bohr magneton, and θ is the angle between the applied magnetic field and the axis of symmetry of the crystalline electric field. For a $^2D_{\frac{3}{2}}$ state under cubic plus tetragonal symmetry, Polder shows[4] that

$$g_{\shortparallel} = 2(1 - 4\lambda/\Delta), \quad g_{\perp} = 2(1 - \lambda/\Delta'), \tag{2}$$
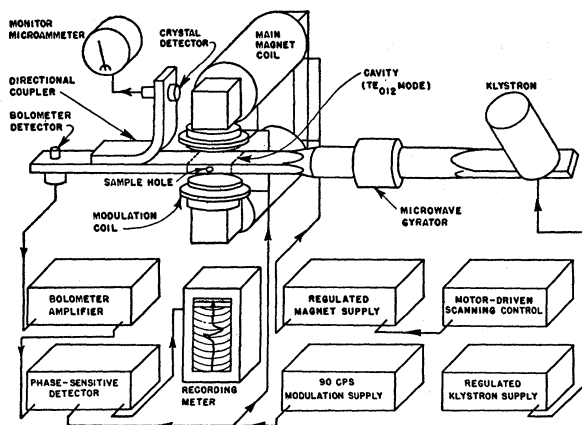

FIG. 1. Block diagram of the microwave absorption spectrometer.

[2] H. Bethe, Ann. Physik **3**, 133 (1929).
[3] H. A. Jahn and E. Teller, Proc. Roy. Soc. (London) **A161**, 220 (1937).
[4] D. Polder, Physica **9**, 709 (1942).

where λ is the spin-orbit coupling constant and Δ and Δ' are the energy differences between the ground state and two higher Stark levels.

The interactions involving the nuclear moment can be written, neglecting the nuclear quadrupole moment, as

$$\mathfrak{IC}_n = g_n \mu_n \mathbf{I} \cdot \mathbf{H} + a \mathbf{L} \cdot \mathbf{I}$$
$$+ b\{3r^{-2}(\mathbf{I} \cdot \mathbf{r})(\mathbf{S} \cdot \mathbf{r}) - \mathbf{I} \cdot \mathbf{S}\} + c \mathbf{I} \cdot \mathbf{S} \tag{3}$$

where c includes the probability that the electron is at the nucleus.[5] Such an interaction when added to the previous interactions yields the energy levels:

$$E_+(M_I) = \tfrac{1}{2} g \mu_B H + \left[\left(\frac{A_{\shortparallel} g_{\shortparallel}}{2g} - g_n \mu_n H \right)^2 \cos^2\theta \right.$$
$$\left. + \left(\frac{A_{\perp} g_{\perp}}{2g} - g_n \mu_n H \right)^2 \sin^2\theta \right]^{\frac{1}{2}} M_I,$$

$$E_-(M_I) = -\tfrac{1}{2} g \mu_B H - \left[\left(\frac{A_{\shortparallel} g_{\shortparallel}}{2g} + g_n \mu_n H \right)^2 \cos^2\theta \right.$$
$$\left. + \left(\frac{A_{\perp} g_{\perp}}{2g} + g_n \mu_n H \right)^2 \sin^2\theta \right]^{\frac{1}{2}} M_I. \tag{4}$$

For a $^2D_{\frac{3}{2}}$ state, if one uses Eq. (2),

$$A_{\shortparallel} = (g_{\shortparallel} - 2)\langle a \rangle + (3/7)(g_{\perp} - 2)\langle b \rangle - (4/7)\langle b \rangle + \langle c \rangle, \tag{5}$$
$$A_{\perp} = (g_{\perp} - 2)\langle a \rangle - (3/14)(g_{\perp} - 2)\langle b \rangle + (2/7)\langle b \rangle + \langle c \rangle.$$

The above five equations are sufficient to describe the resonances reported in detail in this paper. The general shapes of the resonance absorption curves can be obtained by considering the amorphous character of the samples studied, as will be shown.

II. VITREOUS STATE

The physics of glass is complicated by the fact that this vitreous state is not in thermal equilibrium. Rather such a state exists only by virtue of negligible rates of crystallization.

The glasses of interest here are those based on silica. Furthermore, all glass samples employed have been the product of fusing together various oxides. This does not imply that these oxides exist as such in the vitreous state, however. They fulfill certain functional purposes in the glass, two of which are labeled "network-formers" and "network-modifiers," by which is meant that some oxides have a coordination number for the metallic ion which is suitable for forming long oxide "chains," while other oxides present coordination numbers not suitable for such a formation and hence must either allow their metallic ions to fill interstitial positions in the network or join with conjugate oxides

[5] For a comprehensive discussion of the appropriate Hamiltonians see B. Bleaney and K. W. H. Stevens, Repts. Progr. Phys. **16**, 108 (1953).

to form a binary network. In a silica glass these functions demand that a metallic ion either lie inside a tetrahedron of oxygen atoms or rest in an interstitial position where its coordination number may be different from two.

The position which an ion assumes in the glass is of considerable importance since the optical absorption of the ion depends upon its surroundings as noted in Sec. I. In fact, it is just this dependence that is of interest here.

III. EXPERIMENTAL ARRANGEMENT

The apparatus employed in studying the effect of the environment on the ground state spin levels of the paramagnetic ions in the various glasses is outlined in Fig. 1. This paramagnetic resonance (PMR) spectrometer was designed to sweep the applied magnetic field from zero to 5000 gauss while the paramagnetic sample is bathed continuously in electromagnetic radiation at 9000 Mc/sec. The power absorbed by the sample from the radiation bath is detected and recorded *versus* the applied magnetic field.

The circuit consists of a reflex klystron oscillator feeding microwave power through a ferromagnetic isolator (gyrator) into a transmission cavity (operating in the TE_{012} mode) which contains the sample under investigation. The power transmitted by the cavity is carried to a barreter where any change of power results in a change of dc resistance of the barreter. By virtue of a constant direct current furnished to the barreter, this change of resistance manifests itself as a change in voltage across the barreter which is then amplified through an audio-amplifier, fed into a phase-sensitive detector and finally onto an Esterline-Angus recorder. The applied magnetic field is modulated at a ninety-cycle rate and a phase-coherent reference signal is applied to the grids of the phase-sensitive detector switching tube so as to allow only the resonance signal to pass through the time constant across the switching tube.
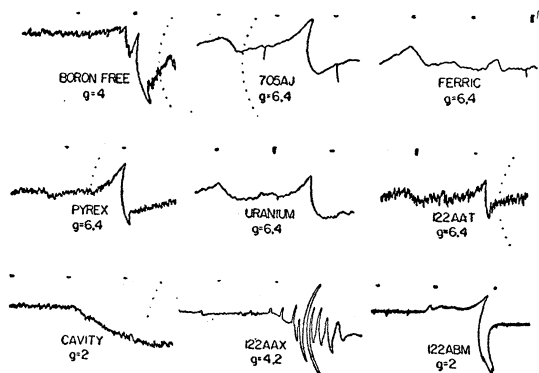

FIG. 2. Representative derivatives of paramagnetic resonance absorption lines in glasses.

The circuit for the magnetic field sweep consists of a constant current supply whose reference voltage may be swept continuously by means of a helipot. The clock motor in the recorder drives both the chart and the reference voltage helipot. The resulting current sweep through the magnet coils is quite linear with time; over the ranges employed in the following experiments, the field sweep is linear as well.

IV. EXPERIMENTAL RESULTS

Figure 2 shows a representative group of derivatives of the paramagnetic resonance absorption curves recorded for the glass samples listed in Table I. In nearly all cases, save where dielectric absorption ruled otherwise, the samples were rectangular sections of 0.5-cm^2 cross-sectional area, extending across the total width of the microwave cavity at a region where the electric field was a minimum. Table I displays the values of the spectroscopic splitting factors (g-values) observed for each sample surveyed. It is of interest to note that in all cases there existed resonances having apparent anisotropic g-values of 4 and 6. That these are anisotropic g-values for a particular paramagnetic impurity in the glasses is, of course, not immediately obvious. However, the shapes of the integrated curves are in good accord with this assumption, as will be shown.

Prior to any computations, one may make a few qualitative remarks. Experiment shows that the spectra observed do not seem to alter upon working the glass. This, perhaps, indicates that impurities are responsible and that nothing analogous to F-centers is operative. Such a conclusion is further substantiated by the fact that for glasses made from the same base, the line intensities remain the same; but for varying bases one finds varying intensities.

Let us suppose that the conditions under which Eq. (1) was derived hold true. Then the energy of a $\Delta m = 1$ transition is given by

$$h\nu = g\mu_B H, \qquad (6)$$

where $g = (g^2_{||} \cos^2\theta + g_{\perp}^2 \sin^2\theta)^{\frac{1}{2}}$ as before. In the glass, however, all orientations of the crystalline field symmetry axis are equally probable, and one must sum over all the absorptions. If one sweeps the applied magnetic field while maintaining the frequency at a constant value ν_0 as was done here, then absorption of energy will occur at fields given by

$$H = (h\nu_0/\mu_B)(g_{||}^2 \cos^2\theta + g_{\perp}^2 \sin^2\theta)^{-\frac{1}{2}}, \qquad (7)$$

for each value of θ.

The number of spins having for their environment an electric field symmetry axis at an orientation with respect to the applied magnetic field between θ and $\theta + d\theta$ is given by

$$dN = (N_0/2) \sin\theta d\theta, \qquad (8)$$

TABLE I. Apparent g-values observed in glasses. The numbers in parentheses indicate the percentage by weight of the individual paramagnetic impurities added to the purest soda-lime-silica base glass available. Resonances marked "Str" show hyperfine structures characteristic of the known paramagnetic additions.

Pyrex	6.2; 4.2	122ABA CuO, TaO, WO₃ (0.4%)	6.0; 4.2; 2(Str)
Nonex	6.4; 4.3	122ABB ZrO, Cb₂O₃ (0.4%) Nd₂O₃, Pr₂O₃ (0.2%)	6.0; 4.2
705AJ	6.0; 4.0	122ABC SnO, YtO, Ce₂O₃	6.0; 4.2
Fused quartz	6.2; 4.2	122ABD TiO₂, V₂O₅ (0.01%)	6.0; 4.2; 2(Str)
Neutron irrad. crystalline quartz	5.0; 4.4	122ABE Mn₂O₃, Cr₂O₃ (0.01%)	6.0; 4.2; 2(Str)
Boron free	6.0; 4.3	122ABF	6.0; 4.2
Lime	6.0; 4.3	122ABG NiO, MoO₃, (0.01%)	6.0; 4.2
Soft glass No. 1	6.0; 4.3	122ABH CuO, TaO, WO₃ (0.01%)	6.0; 4.2; 2(Str)
Cobalt	7.0; 4.4	122ABI ZrO (0.01%) Nd₂O₃, Pr₂O₃ (0.005%)	6.0; 4.2
Uranium	6.0; 4.2	122ABJ SnO, Ce₂O₃, YtO (0.01%)	6.0; 4.2
122AAT ordinary base materials	6.0; 4.2	122ABK Fe₂O₃ (0.01%)	6.0; 4.2
122AAU As₂O₃ plus sulfates	6.0; 4.2	122ABL	6.0; 4.2
122AAV As₂O₃	6.0; 4.2	122ABM CuO (0.4%)	6.0; 4.2; 2(Str)
122AAW sulfates	6.0; 4.2	122ABN WO₃ (0.4%)	6.0; 4.2
122AAX TiO₂, V₂O₅ (0.4%)	6.0; 4.2; 2(Str)	122ABO TaO (0.4%)	6.0; 4.2
122AAY Mn₂O₃, Cr₂O₃ (0.4%)	6.0; 4.2; 2(Str)	122ABP pure lime, ordinary sand	6.0; 4.2
122AAZ NiO, MoO₃, (0.4%)	6.0; 4.2; 2(Str)	122ABQ pure sand, ordinary lime	6.0; 4.2

which becomes, from Eq. (7),

$$dN = (N_0/2)(4H_0^2/H^3)$$
$$\times \{(g_{\rm II}^2 - g_\perp^2)[(2H_0/H)^2 - g_\perp^2]\}^{-\frac{1}{2}} dH, \quad (9)$$

where $H_0 = h\nu_0/2\mu_B$.

Figure 3 shows dN/dH from Eq. (9) plotted *versus* H together with an integrated curve obtained for 705AJ (the derivative curve from which this was taken is that shown in Fig. 2). If one allows the individual lines whose centers are distributed according to dN/dH to have a finite width, the agreement between theory and experiment can be made quite satisfactory.

The assumption that these lines are due to an as yet undetermined impurity having anisotropic g-values ($g_\perp \approx 4$ and $g_{\rm II} \approx 6$) in its lattice site in glass appears to be consistent with experiment. It remains, perhaps, to demonstrate that such g-values can be expected to exist. The cobalt ion furnishes the best example. It has been observed to have values between 2.5 and 3.5 for $g_\perp$ and between 5.5 and 7 for $g_{\rm II}$. In glass in relatively large concentration, it shows a $g_\perp$ of 4.4 and a $g_{\rm II}$ of 7 as noted in Table I. Further experimentation is needed, however, to identify the paramagnetic impurity observed here.§

V. CUPRIC ION RESONANCE IN GLASS

In addition to the resonances near $g=4$ and 6 which occurred in all glass samples, there were resonances located near $g=2$ which were characteristic of the known added paramagnetic impurities. An example of these resonances is that for Cu^{2+} in a lattice-modifying position in a soda-lime-silica base glass. The sample employed was labeled 122ABM, and its spectrum is recorded in Fig. 2. Figure 4 shows this derivative

§ *Note added in proof.*—H. Weaver, Varian Associates, has informed the author that an increase in intensity of this anisotropic absorption has been observed in a soda lime glass containing 0.4% Fe_2O_3. This implies that Fe^{+++} may be responsible for these lines in all the samples studied but Fe^{++} is perhaps more likely.

curve on rectangular coordinates together with its integrated absorption curve. One notes how much more sensitive the derivative is to structure than is its integrated counterpart. It shows two sets of four equally spaced peaks—one set centered about 2770 gauss and the other about 3130 gauss with considerably different spacings. From Sec. I, the conditions of a large Stark splitting of the orbital levels ($^2D_{\frac{5}{2}}$) together with a spin-orbit coupling and nuclear hyperfine interactions seem to fit the data.

Equations (4) and (5) were derived under these assumptions, neglecting the nuclear quadrupole moment. If one also neglects $g_n\mu_nH$ relative to $A_{\rm II}/2$ and $A_\perp/2$, then

$$h\nu_{\frac{1}{2}\to-\frac{1}{2}} = g\mu_B H + 2M_I(g_{\rm II}^2 \cos^2\theta + g_\perp^2 \sin^2\theta)^{-\frac{1}{2}}$$
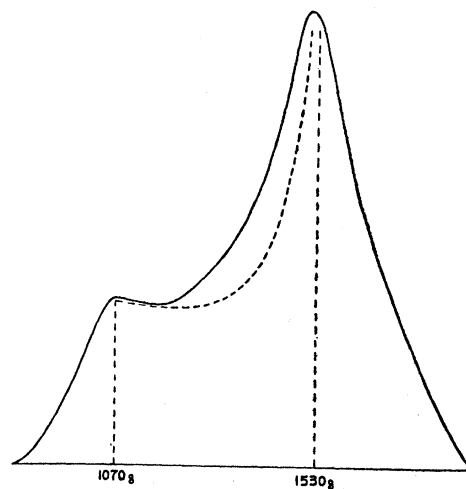$$\times (d^2 \cos^2\theta + f^2 \sin^2\theta)^{\frac{1}{2}}, \quad (10)$$

FIG. 3. Theoretical and experimental absorption curves for glass sample 705AJ. The dashed curve represents the plot of the theoretical distribution of line centers [dN/dH of Eq. (9)] *versus* H. The solid curve is the integrated absorption curve from a sample of 705AJ glass.
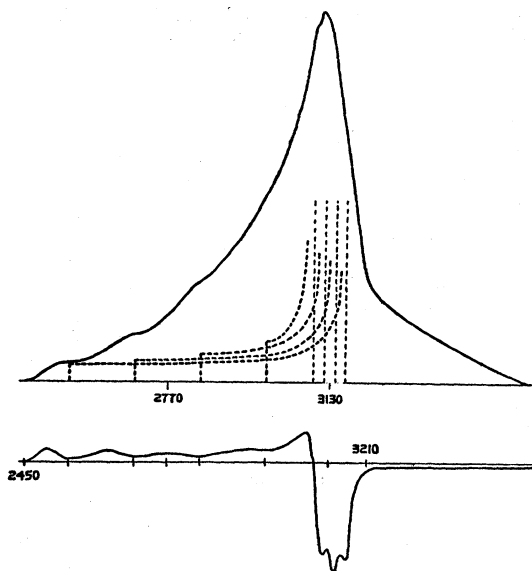
FIG. 4. Derivative and integrated absorption curves for Cu^{2+} in a lattice-modifying position in a soda-lime-silica base glass. The dashed curves are the theoretical line center distributions from Eqs. (8) and (11).

with $d = A_{||}g_{||}/2$ and $f = A_{\perp}g_{\perp}/2$. Defining $h\nu_0 = 2\mu_B H$,

$$H = 2H_0/g - 2M_I\mu_B^{-1}(g_{||}^2\cos^2\theta + g_{\perp}^2\sin^2\theta)^{-1}$$
$$\times (d^2\cos^2\theta + f^2\sin^2\theta)^{\frac{1}{2}}, \quad (11)$$

again, one expects that the axes of the Stark fields at the ion sites in the glass will be randomly oriented. As before, one may plot dN/dH versus H. The upper and lower limits in field are

$$H_U = 2H_0/g_{\perp} - 2Mf/g_{\perp}^2\mu_B, \quad (12)$$
$$H_L = 2H_0/g_{||} - 2Md/g_{||}^2\mu_B,$$

and these clearly fulfill the condition of two sets of equally spaced lines as shown in Fig. 4. If one now refers to the experimental curves, one notes that the most intense absorption occurs at the lower field value in the set of lines centered about 3130 gauss. Since all nuclear spin orientations can be treated as equally likely, this means that the relative signs of the parameters d and f must be opposite. This is in agreement with what one considers probable. That is, from Eq. (3) one sees that the parameters a and b are functions of the radial coordinate and that

$$a = b = g_n g\mu_n\mu_B/r^3. \quad (13)$$

From Eq. (5) and the assumption of no s-state promotion,

$$A_{||} = [(g_{||}-2)+3(g_{\perp}-2)/7-4/7]\langle a \rangle,$$
$$A_{\perp} = [(g_{\perp}-2)-3(g_{\perp}-2)/14+2/7]\langle a \rangle. \quad (14)$$

Taking the values $g_{||} = 2.32$ and $g_{\perp} = 2.06$ from Fig. 4, one obtains $A_{||} = -0.23\langle a \rangle$ and $A_{\perp} = 0.33\langle a \rangle$. Thus, from Eq. (10) one might expect the parameters d and f to have opposite signs since the amount of promotion is certainly small.

From Fig. 4 and the preceding definitions one finds $g_{||} = 2.32$, $g_{\perp} = 2.06$, $d = -548$ Mc/sec and $f = 72.6$ Mc/sec. These data demand that $\langle c \rangle$ in Eq. (5) be negative. If one defines κ by the equation $\langle c \rangle = -\kappa\langle a \rangle$, then one obtains

$$A_{||} = -(\kappa + 0.23)\langle a \rangle,$$
$$A_{\perp} = (0.33 - \kappa)\langle a \rangle. \quad (15)$$

From the values for d and f one finds $\kappa = 0.26$. These experimental values are in excellent accord with the results reported for copper in the Tutton salts.[6,7]

CONCLUDING REMARKS

These resonances show clearly that there is definite short-range order in the lattice-modifying positions of many glasses, and the ability to investigate the symmetry of the individual lattice positions in the vitreous state should be of considerable aid to the glass technologist. With higher impurity content, resonances not reported for paramagnetic ions in Table I have become observable.[8]

The hyperfine structure observed for the titanium-vanadium loaded sample (122AAX) has been recorded for a vanadium loaded sample alone. Resonance studies on vanadium ions in solution indicate that the strong central absorption is due to vanadium ions in one lattice site while the eight-line spectrum is attributable to vanadium ions in another site. Whether these are also different ionization states has not been determined. The central absorption grows in the liquid state as the concentration of the vanadium salt is increased. Theoretical work is underway in an attempt to explain the width variation of the individual lines of the eight-line spectrum recorded in solution, and this should shed considerable light on the spectrum noted here in glass. The results of this latter work will be published shortly.

[6] Bleaney, Penrose, and Plumpton, Proc. Roy. Soc. (London) A198, 406 (1949).
[7] A. Abragam and M. H. L. Pryce, Proc. Roy. Soc. (London) A206, 164 (1951).
[8] H. Weaver (private communication).